crystals

MDPI

Article

Fabrication and Optical Properties of 2at.%Yb:LuYAG Mixed Crystal through Nanocrystalline Powders

Ding Zhou [1], Meiqi Yang [1], Jiayue Xu [1,*], Yijian Jiang [2], Yunfeng Ma [1,2] and Ying Shi [3,*]

[1] Institute of Crystal Growth, School of Materials Science and Engineering, Shanghai Institute of Technology, Shanghai 201418, China; dzhou@sit.edu.cn (D.Z.); mqyang@sit.edu.cn (M.Y.); yunfengma@sit.edu.cn (Y.M.)
[2] Institute of Laser Engineering, Beijing University of Technology, Beijing 100124, China; yjjiang@bjut.edu.cn
[3] School of Material Science and Engineering, Shanghai University, Shanghai 20072, China
* Correspondence: xujiayue@sit.edu.cn (J.X.); Yshi@shu.edu.cn (Y.S.); Tel.: +86-021-6087-3439 (J.X.); +86-021-3633-8410 (Y.S.)

Received: 7 September 2018; Accepted: 5 November 2018; Published: 8 November 2018

Abstract: Ytterbium doped $Lu_{1.5}Y_{1.5}Al_5O_{12}$ (LuYAG) nanocrystalline powders were synthesized by a wet chemical mixed precipitant co-precipitation (MPP) method, and then the mixed crystal of Yb:LuYAG was grown in an optical floating zone (OFZ) furnace at the speed of 6–10 mm/h, using a [111] oriented YAG seed crystal. The transmittance of the polished LuYAG crystal is close to the ideal value of LuAG or YAG. The X-ray rocking curve shows complete symmetry and the full width at half maximum (FWHM) is 10 arc-second, indicating the good quality of as grown Yb:LuYAG multicomponent garnet crystal. The thermal luminescent spectrum at room temperature shows four deep energy traps at around 1–1.3 eV. X-ray excited luminesce (XEL) spectra is measured to characterize the existence of Lu_{Al} or Y_{Al} shadow defects in the bulk single crystal. The emission peak at around 320 nm indicates that the LuYAG crystal prepared by OFZ have lower concentrations of antisite defects (AD) with respect to its Czochralski counterpart.

Keywords: crystal growth; LuYAG; optical floating zone; optical properties

1. Introduction

Compared with YAG host material, lutetium aluminum garnet ($Lu_3Al_5O_{12}$, LuAG) is characterized by favorable properties such as high Zeff, high density, high doping concentrations and outstanding thermal conductivity [1–4]. Because of the above advantages, LuAG host materials were widely used in solid state lasers and scintillators in transparent ceramics and crystals [5–8].

LuAG crystals usually grown by the traditional crystal growth processing such as Czochralski (CZ), Bridgman, or the other techniques. However, the high melting point of LuAG (2010 °C) and the long growth cycles make it easy to introduce Lu_{Al} AD in the crystal, which will affect the optical performances of crystals, especially as scintillators [4]. To reduce the concentration of AD in LuAG crystals, one way is to lower the melting point by introducing the component of low melting point YAG, and the other way is to accelerating the growth speed. That is the motivation we develop LuYAG mixed crysals by OFZ. In 2004, Kuwano et al. first used a solar furnace to determine solidification points of LuYAG, and then grew LuYAG crystals by CZ method [9]. They investigated the solidification point, the lattice parameter, the thermal conductivity, and refractive index of a series $(Lu,Y)_3Al_5O_{12}$ in details. The melting point of the $Lu_{1.5}Y_{1.5}Al_5O_{12}$ crystal is 40 °C lower than that of LuAG crystal [9]. In recent years, the spectroscopic properties of LuYAG mixed crystal doped with different rare earth ions were widely studied. In our review of the published literatures, the LuYAG mixed crystals were grown by Czochralski or μ-pulling down (μ-PD) method [10–13].

In this paper we report, for the first time to our knowledge, the growth of optical grade Yb:LuYAG mixed crystals by using MPP derived nanocrystalline LuYAG powders, combined with optical floating zone method, using YAG seed crystal. The growth speed is 6–8 times faster than the CZ method. The detailed results concerning crystal growth and the optical properties are also discussed.

2. Materials and Methods

2.1. Powder Synthesis

The Yb doped LuYAG powders were synthesized by a modified wet chemical method, using ammonium hydroxide and ammonium hydrogen carbonate as the mixed precipitator as reported in our previous works [14–16]. The starting chemicals used were commercial high purity powders without further purification: lutetium oxide (Lu_2O_3, 4N5), yttrium oxide (Y_2O_3, 4N5), ytterbium oxide (Yb_2O_3, 4N5), nitric acid (HNO_3, GR), aluminum nitrate ($Al(NO_3)_3$, AR), ammonium hydrogen carbonate (NH_4HCO_3, AR), and ammonium hydroxide (NH_4OH, AR). Aqueous solution of (Lu^{3+}, Y^{3+}, Yb^{3+}, Al^{3+}) were prepared by dissolving these solid powders into hot HNO_3 or deionized water, following the formula 2at.%Yb:$Lu_{1.5}Y_{1.5}Al_5O_{12}$. Finally, Yb-doped LuYAG precursors were synthesized by reverse-strike co-precipitant method. After aged and calcined, the nanocrystalline powders were used to make the feed rods for crystal growth by optical floating zone method.

2.2. Crystal Growth

Yb:LuYAG mixed crystals were grown in an optical floating zone (OFZ) furnace (Crystal Systems Inc., Salem, MA, USA, FZ-T-12000-X-I-S-SU) equipped with four 3 kW Xenon lamps reaching a maximum temperature of 3000 °C (100% lamp power). The single crystal was grown along the [111] direction, utilizing pure YAG with [111] direction as the seed crystal. Argon gas, 30 mL/min flow, was introduced into the growth chamber as for the protective atmosphere. In the process of crystal growth, the crystal growth rate and feed rod feeding speed needs to be accurately controlled, in order to keep the as-grown LuYAG mixed crystal in the same diameter. In this paper, the optimized parameter of the growth rate was kept in the range of 6–10 mm/h, and the rotation rates of the feed rod and the seed rod were both maintained at 15 rpm in opposite directions. After the growth was finished, the crystal was cooled down to room temperature at the speed of 600 °C/h. The growth technology and the detailed procedure of OFZ method can be found in references [17,18].

2.3. Measurements

Thermal decomposition behaviors of the precursor powder were characterized on TG-DSC apparatus (STA 449 F3, NETZSCH, Selb, Bavaria, Germany). Phase composition identification was performed with X-ray diffractometer (Dmax-2550, Rigaku, Japan) equipped with graphite monochromatized Cu Kα radiation (λ = 1.5406 Å, 40 kV/200 mA) in the range of 2θ = 10–80°. Photo-luminescent spectra were measured using spectrophotometer (PL, Ed, England). Thermally stimulated luminescence (TSL), equipped by a Harshow 2000 TL reader was measured to investigate the trap energy level at a heating rate of 5 °C/s. X-ray excited luminescence (XEL) spectra were measured on a home-made X-ray excited luminescence spectrometer, X-ray tube (70 kV × 2.5 mA). All measurements were carried out at room temperature.

3. Results and Discussion

Figure 1 shows the thermogravimetric-differential scanning calorimeter (TG-DSC) curves of the precursor derived from a modified wet chemical precipitant. In the curves, the precursor reveals a continuous thermal decomposition from room temperature till 1100 °C with a total weight loss of about 37%. The DSC curves show that the endothermic peak at 119 °C resulted from the release of OH^- in precursors. The wide band of exothermic peak located at around 405 °C corresponds to the decomposition of CO_3^{2-}. It can be inferred that the exothermic peaks at about 890 °C, 936 °C and

1026 °C resulted from the phase formations of the $Lu_{0.5}Y_{0.5}AlO_3$ (LuYAP), $Lu_2Y_2Al_2O_9$ (LuYAM), and LuYAG, respectively [19]. Compared to the solid-state reaction synthesis, the LuYAG phase formed at a much lower temperature of about 1026 °C (solid state synthesis: over 1400 °C). What is more, the much lower synthesis temperature indicates a better reactivity of the LuYAG nanocrystalline powder. It is favorable for the melting of the feed rod used in optical floating zone furnace.

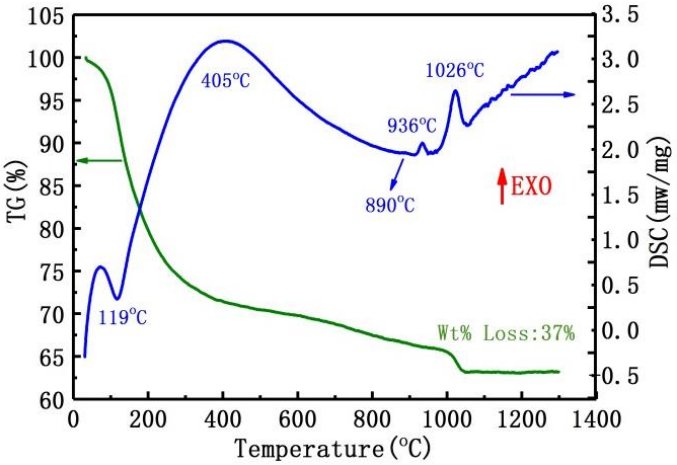

Figure 1. Thermogravimetric-differential scanning calorimeter (TG-DSC) curves of the as synthesized Yb:LuYAG precursors.

X-ray diffraction (XRD) patterns of Yb:LuYAG powders (calcined at 1100 °C/2 h) are shown in Figure 2a. The patterns exhibit a cubic garnet phase and no other impurity phases are detected. The main characteristic peaks are in good agreement with the standard PDF cards (LuAG JCPDS:73–1368 and YAG JCPDS:72–1315). The X-ray rocking curves with (444) direction show complete symmetry and the full width at half maximum (FWHM) is a 10 arc-second, indicating that the Yb:LuYAG mixed crystals have good optical quality, as shown in Figure 2b.

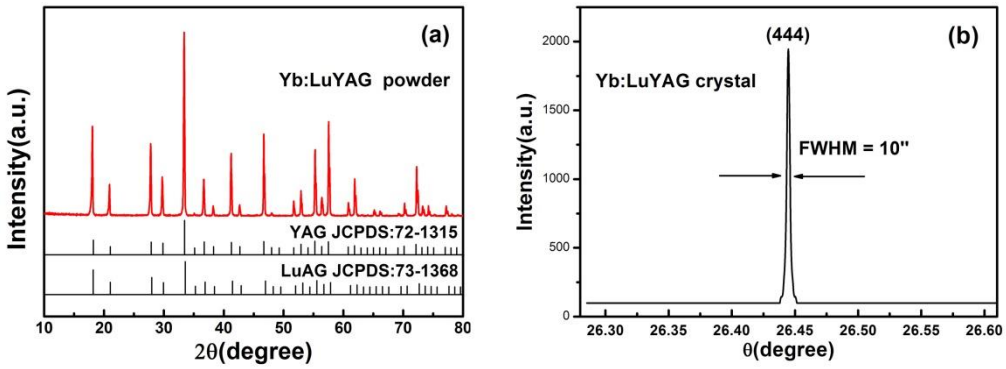

Figure 2. (**a**) X-ray diffraction (XRD) of Yb:LuYAG polycrystal powder and (**b**) the X-ray rocking curve.

Figure 3 shows the optical transmittance of Yb:LuYAG crystal, polished on both sides (1.2 mm in thickness) in the wavelengths that range from 200 to1500 nm. From the transmittance curve, it can be seen that the linear transmittance increases from 82% to 83.5% in the range of 400–800 nm wavelength, and the transmittance has been maintained at around 84% in the infrared range (800–1500 nm). The absorption bands at 912, 937, 965, and 1027 nm wavelengths are caused by Yb-ions in the measurement wavelength. The high optical transmittance indicates that the optimized MPP nanocrystalline powder coupled with the optical floating zone method could be a promising route for preparing optical grade LuYAG crystals. The inset is the appearance of as-grown Yb:LuYAG single crystals in the dimension of about Φ 5 $\times$ 40 mm.

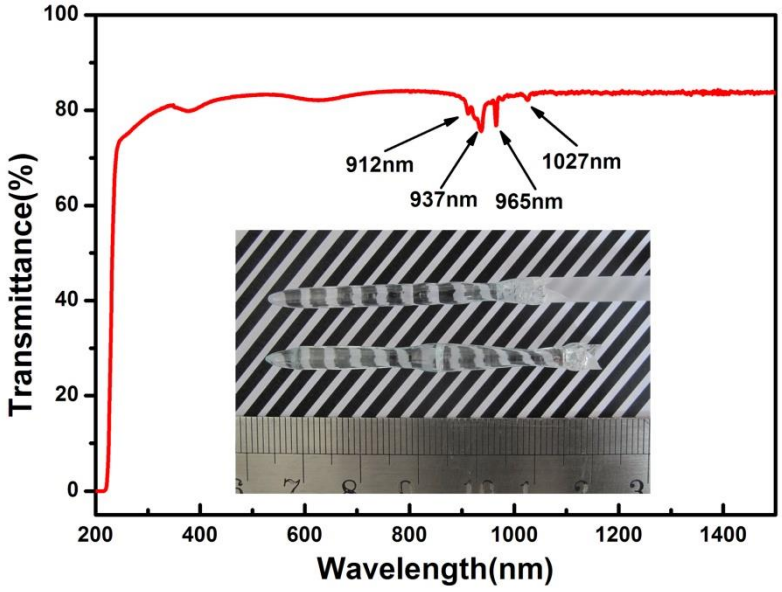

Figure 3. In-line transmittance of LuYAG crystals (inset: appearance of as-grown crystal).

Figure 4 shows the room temperature excitation and emission spectra of LuYAG crystal doped by ytterbium activators. The main emission peak is centered at 1030 nm, corresponding to the transition of ^{2}F5/2–^{2}F7/2. when excited at 969 and 940 nm wavelength respectively. From the emission spectrum, the intensity excited at 940 nm is about 1.3 times of that excited at 969 nm because of the larger excitation peak areas at 940 nm.

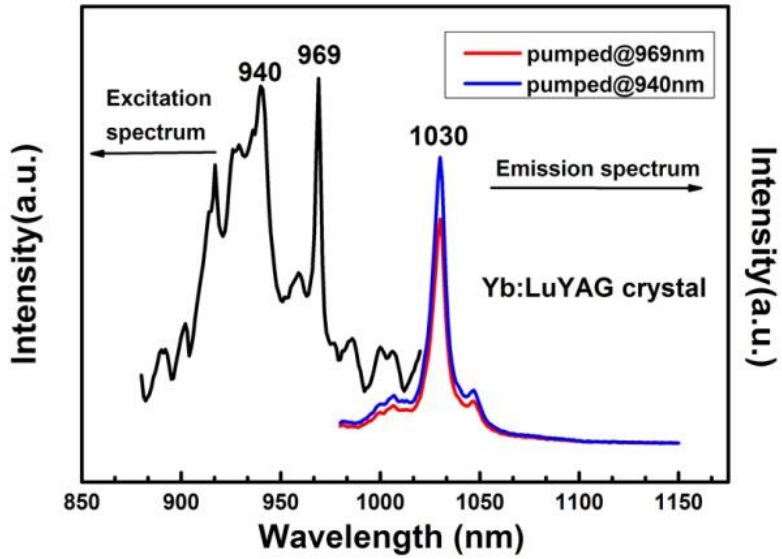

Figure 4. Fluorescence spectrum of Yb:LuYAG crystal.

Thermo-luminescence (TL) is an effective technique for the investigation of possible presence and distribution of traps in materials. To figure out the crystal quality and the luminescence potential of the as-grown mixed crystals, TSL was conducted on the Yb:LuYAG mixed crystal, as shown in Figure 5. In our experiment, the crystal was irradiated for 60 min by a home-made UV irradiation instrument, and then the TSL glow curves above room temperature were measured by a Harshow 2000 TL reader (heating rate: 5 °C/s). A resultant curve was fitted using the general order kinetics equation [20,21]. The values of the trap parameters of the trap energy level and the concentration of trapped charges (n_0) are shown in Table 1.

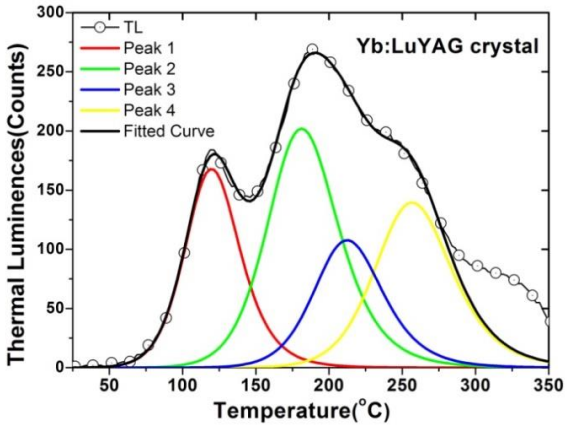

Figure 5. Thermal luminescence glow curves of Yb:LuYAG single crystal.

Table 1. Thermally stimulated luminescence (TSL) parameters from the curve fitting.

Peak	Peak Temperature (°C)	Trap Energy (eV)	n_0
Peak 1	120	0.998	1687.18
Peak 2	181	1.028	2613.49
Peak 3	212	1.218	1353.02
Peak 4	257	1.296	1957.89

The result shows that there are four TL peaks from room temperature to 300 °C and the trap depth value of as-grown Yb:LuYAG crystal are around 1–1.3 eV. In order to further characterize the shallow level defects (such as antisite defect of Lu_{Al}), the XEL spectra of the OFZ and CZ LuYAG crystal are measured at room temperature, as shown in Figure 6. The CZ crystal shows an obvious higher emission peak than that of OFZ crystal around 320 nm, which is ascribed to the existence and concentration of Lu_{Al} antisite defects in the mixed LuYAG hosts [21]. In general, the antisite defect is a kind of common defect in high meting point crystals. However, in this paper, MPP and OFZ fabricated Yb:LuYAG crystal demonstrates a lower XEL peak at 320 nm than that of the CZ counterpart. To our knowledge, the high melting point of LuAG (2010 °C) and the long growth cycles make it easy to introduce Lu_{Al} AD in the crystal. The mechanism of reducing the concentration of AD in LuAG crystals are suggested as (1) Y-ions was doped into LuAG (to form $Lu_{1.5}Y_{1.5}Al_5O_{12}$ mixed crystal) to lower the melting point of about 40 °C respect to LuAG crystal; (2) Shortening of the growth cycle leads to an acceleration of the crystal growth process. Thus, the fast speed growth route of OFZ is adopted; (3) High reactivity LuYAG nanocrystalline powders synthesized by MPP, which is supported as the key feed rod used for the OFZ crystal growth at a fast speed.

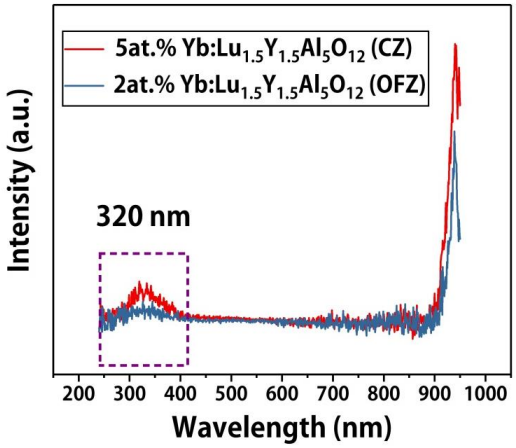

Figure 6. X-ray excited emission spectrum at room temperature.

4. Conclusions

We have successfully synthesized the MPP derived nanocrystalline powders for preparing a dense Yb:LuYAG feed rod, which is a key factor to grow LuAG crystal. By the OFZ method, crack-free Yb:LuAG crystals with a dimension of Φ 5 $\times$ 40 mm were grown with the optimized conditions of the growth rate of 6–10 mm/h and the rotation rate of 15 rpm. The narrow FWHM of 10 arc-second and high optical transmittance of 83.5% reveal good optical quality of our OFZ crystal. The thermal luminescent spectrum at room temperature shows four deep energy traps at around 1–1.3 eV. X-ray excited luminesce (XEL) spectra is measured to characterize the existence of Lu_{Al} or Y_{Al} shadow defects in the bulk single crystal. The lower X-ray excited emission intensity at 320 nm of OFZ crystal shows that there are less antisite defects in OFZ crystal than that in CZ grown counterpart, and the mechanism was suggested.

Author Contributions: Data curation, D.Z. and Y.M.; Writing—original draft preparation, D.Z.; writing—review and editing, M.Y.; funding acquisition, Y.S., J.X. and Y.J.

Funding: This research was funded by National Natural Science Foundation of China, grant number 51472263, 21875138, U1732128 and Shanghai innovation action plan project (15520503400).

Acknowledgments: The authors show their acknowledgement to Zhengye Xiong from Guangdong Ocean University for the helpful discussions and TSL spectra measurements. We also thank Xiaodong Xu from Shanghai institute of ceramics for offering us CZ grown Yb:LuYAG single crystal.

Conflicts of Interest: The authors declare no conflict of interest. The funders had no role in the design of the study; in the collection, analyses, or interpretation of data; in the writing of the manuscript, and in the decision to publish the results.

References

1. Sato, Y.; Akiyama, J.; Akiyama, T.; Taira, T. Effects of rare-earth doping on thermal conductivity in $Y_3Al_5O_{12}$ crystals. *Opt. Mater.* **2009**, *31*, 720–724. [CrossRef]
2. Griebner, U.; Petrov, V. Passively mode-locked Yb:Lu_2O_3 laser. *Opt. Express* **2004**, *12*, 3125–3130. [CrossRef] [PubMed]
3. Jiang, B.X.; Lu, X.; Zeng, Y.P.; Liu, S.P.; Li, J.; Liu, W.B.; Shi, Y.; Pan, Y.B. Synthesis and properties of Yb:LuAG transparent ceramics. *Phys. Status Solidi C* **2013**, *10*, 958–961. [CrossRef]
4. Nikl, M.; Yoshikawa, A.; Kamada, K.; Nejezchleb, K.; Stanek, C.R.; Mares, J.A.; Blazek, K. Development of LuAG-based scintillator Crystals-A review. *Prog. Cryst. Growth Charact.* **2013**, *59*, 47–72. [CrossRef]
5. Luo, D.W.; Zhang, J.; Xu, C.W.; Yang, H.; Lin, H.; Zhu, H.Y.; Tang, D.Y. Yb:LuAG laser ceramics: a promising high power laser gain medium. *Opt. Mater. Express* **2012**, *2*, 1425–1431. [CrossRef]
6. Beil, K.; Thornton, S.T.; Tellkamp, F.; Peters, R.; Kränkel, C.; Petermann, K.; Huber, G. Thermal and laser properties of Yb:LuAG for kW thin disk lasers. *Opt. Express* **2010**, *18*, 20712–20722. [CrossRef] [PubMed]
7. Raghavan, R.S. New Prospects for Real-Time Spectroscopy of Low Energy Electron Neutrinos from the Sun. *Phys. Rev. Lett.* **1997**, *78*, 3618–3621. [CrossRef]
8. Antonini, P.; Bressi, G.; Carugno, G.; Iannuzzi, D. Scintillation properties of YAG:Yb crystals. *Nucl. Instrum. Methods Phys. Res. A* **2001**, *460*, 469–471. [CrossRef]
9. Kuwano, Y.; Suda, K.; Ishizawa, N.; Yamada, T. Crystal growth and properties of $(Lu,Y)_3Al_5O_{12}$. *J. Cryst. Growth* **2004**, *260*, 159–165. [CrossRef]
10. Di, J.Q.; Xu, X.D.; Xia, C.T.; Li, D.Z.; Zhou, D.H.; Wu, F.; Xu, J. Crystal growth and optical properties of LuYAG: Ce single crystal. J. *Cryst. Growth* **2012**, *351*, 165–168. [CrossRef]
11. Zhang, H.L.; Sun, D.L.; Luo, J.Q.; Fang, Z.Q.; Zhao, X.Y.; Cheng, M.J.; Zhang, Q.L.; Yin, S.T. Growth and spectroscopic properties of the 2.9 mum Tm, Ho:LuYAG laser crystals. *Opt. Mater.* **2015**, *47*, 490–494. [CrossRef]
12. Niu, X.J.; XU, J.Y.; Zhou, D.; Wang, S.X.; Zhang, H.J. Synthesis and Growth of Ce,Pr:YLuAG Crystal for LED Application. *J. Inorg. Mater.* **2015**, *30*, 1181–1186.
13. Drozdowski, W.; Brylew, K.; Wojtowicz, A.J.; Kisielewski, J.; Świrkowicz, M.; Łukasiewicz, T.; Haas, J.T.; Dorenbos, P. 33000 photons per MeV from mixed $(Lu_{0.75}Y_{0.25})_3Al_5O_{12}$:Pr scintillator crystals. *Opt. Mater. Express* **2014**, *4*, 1207–1212. [CrossRef]

14. Xu, J.; Shi, Y.; Xie, J.J.; Lei, F. Fabrication, microstructure, and luminescent properties of Ce^{3+}-doped $Lu_3Al_5O_{12}$ (Ce:LuAG) transparent ceramics by low-temperature vacuum sintering. *J. Am. Ceram. Soc.* **2013**, *96*, 1930–1936. [CrossRef]
15. Zhou, D.; Shi, Y.; Yun, P.; Xie, J.J. Effects of precipitants on morphologies and properties of Nd^{3+}:Lu_2O_3 nanopowders prepared by a wet chemical processing. *J. Alloy. Compd.* **2009**, *479*, 870–874. [CrossRef]
16. Zhou, D.; Shi, Y.; Xie, J.J.; Chen, D.M.; Dong, J.; Ueda, K.; Xu, J.Y. Laser grade Yb:LuAG transparent ceramic prepared by nanocrystalline pressure-less sintering in reducing H_2. *Opt. Mater. Express* **2017**, *7*, 1274–1280. [CrossRef]
17. Koohpayeh, S.M.; Fort, D.; Abell, J.S. The optical floating zone technique: A review of experimental procedures with special reference to oxides. *Prog. Cryst. Growth Charact.* **2008**, *54*, 121–137. [CrossRef]
18. Tian, L.; Wang, S.X.; Wu, K.; Wang, B.L.; Yu, H.H.; Zhang, H.J.; Cai, H.Q. Thermal, spectroscopic and laser properties of Nd^{3+} in gadolinium scandium gallium garnet crystal produced by optical floating zone method. *Opt. Mater.* **2013**, *36*, 521–528. [CrossRef]
19. Li, J.G.; Ikegami, T.; Lee, J.H.; Mori, T. Characterization of yttrium aluminate garnet precursors synthesized via precipitation using ammonium bicarbonate as the precipitant. *J. Mater. Res.* **2000**, *15*, 2375–2386. [CrossRef]
20. McKeever, S.W.S.; Moscovitch, M.; Townsend, P.D. *Thermoluminescence Dosimetry Materials: Properties and Uses*; Nuclear Technology Publishing: Ashford, UK, 1995; ISBN 1-870965-19-1.
21. Nikl, M.; Mihokova, E.; Pejchal, J.; Vedda, A.; Zorenko, Y.; Nejezchle, K. The antisite Lu_{Al} defect-related trap in $Lu_3Al_5O_{12}$:Ce single crystal. *Phys. Stat. Sol. (b)* **2005**, *242*, R119–R121. [CrossRef]